Photonic eigenmodes and light propagation in periodic structures of chiral nanoparticles

A. Christofi,[1,2,*] N. Stefanou,[1] and G. Gantzounis[3]

[1]*University of Athens, Section of Solid State Physics, Panepistimioupolis, GR-157 84 Athens, Greece*

[2]*Institute of Materials Science, NCSR "Demokritos," GR-153 10 Athens, Greece*

[3]*Institute of Microelectronics, NCSR "Demokritos," GR-153 10 Athens, Greece*

(Received 10 February 2011; revised manuscript received 12 April 2011; published 27 June 2011)

We present a detailed analysis of the optical modes and light propagation in photonic crystals consisting of chiral spheres in a nonchiral isotropic medium, calculated by the full electrodynamic layer-multiple-scattering method. It is shown that resonant modes of the individual spheres give rise to narrow bands that hybridize with the extended bands of the appropriate symmetry associated with light propagation in an underlying effective chiral medium. The resulting photonic dispersion diagrams exhibit remarkable features, peculiar to a system that possesses time-reversal but not space-inversion symmetry, which are analyzed in terms of group theory. In particular, we reveal the occurrence of strong band bending away from the Bragg points with consequent negative-slope dispersion inside the first Brillouin zone, slow-photon bands, and frequency gaps. The calculated band structure is discussed in conjunction with relevant reflection diagrams, providing a consistent interpretation of the underlying physics.

DOI: 10.1103/PhysRevB.83.245126 PACS number(s): 42.70.Qs, 42.25.Bs, 78.20.Ek, 33.55.+b

I. INTRODUCTION

Photonic crystals consisting of chiral building units periodically arranged in one, two, and three dimensions have been investigated during the past decades, mainly in relation to the occurrence of frequency band gaps.[1–3] More recently, it has been suggested that material chirality offers new opportunities to realize negative refraction and related effects in effectively uniform media. Specifically, it has been shown that the existence of a chiral resonance, realized either in a mixture of small helical inclusions[4,5] or in an assembly of resonant particles in a nondispersive chiral medium,[6] leads to negative refraction and superlensing for one polarization, resulting in improved and simplified designs of novel chiral optical metamaterials.[7–12] Furthermore, in the strong-chirality regime, intriguing wave properties, such as chirality-dependent node switching, polarization-sensitive transmission, and handedness-dependent mode localization, have been reported on two-dimensional photonic structures consisting of infinite cylinders made of a chiral (meta)material embedded in a dielectric background.[13]

On the other hand, in photonic crystals formed by optically active constituents, the combined effect of space-inversion symmetry breakdown and gyrotropy has the same impact on the eigenmode structure and configuration as in the spin-orbit coupling in electronic band states in asymmetric semiconducting compounds, which allows one to draw certain parallels between electron spin and photospin transport in these periodic structures. Such an analysis was carried out on a one-dimensional chiral/nonchiral periodic multilayer structure in the weak-chirality regime.[14]

In the present work, we report a rigorous group-theory analysis to explain general features of the frequency band structure of three-dimensional photonic crystals consisting of chiral spheres in a nonchiral (dielectric) medium in the strong-chirality regime but below the negative-index threshold, and provide a consistent interpretation of the physical origin of the different eigenmodes of the electromagnetic (EM) field in such structures in conjunction with relevant reflection spectra. The remaining of the paper is organized as follows. Section II summarizes the basic concepts and formulas of electrodynamics in a homogeneous chiral medium. In Sec. III we discuss EM scattering by a single chiral sphere in a homogeneous dielectric medium and, in particular, the particle resonances. In Sec. IV we report a comprehensive analysis of photonic dispersion diagrams and corresponding reflection spectra of a face-centered cubic (fcc) crystal of chiral spheres, calculated by the full electrodynamic layer-multiple-scattering method. The main results of the article are summarized in the last section.

II. ELECTROMAGNETIC WAVES IN A HOMOGENEOUS CHIRAL MEDIUM

The optical response of a homogeneous optically active (chiral) medium is described by the phenomenological Drude-Born-Fedorov constitutive relations[15]

$$\mathbf{D}(\mathbf{r},t) = \epsilon_c\epsilon_0[\mathbf{E}(\mathbf{r},t) + \beta_c\nabla\times\mathbf{E}(\mathbf{r},t)], \tag{1}$$

$$\mathbf{B}(\mathbf{r},t) = \mu_c\mu_0[\mathbf{H}(\mathbf{r},t) + \beta_c\nabla\times\mathbf{H}(\mathbf{r},t)], \tag{2}$$

in which the nonlocal character is reflected by the presence of the spatial derivative (rotation), being a consequence of the EM induction. The dimensionless coefficients ϵ_c and μ_c correspond to the isotropic relative permittivity and permeability, respectively, while the chirality parameter β_c (in units of length) is a real number in a lossless medium. If harmonic time dependence $\exp(-i\omega t)$ is assumed, the field equations for the chiral medium can be compactly written in a matrix form[15]

$$\nabla^2\begin{pmatrix}\mathbf{E}\\ \mathbf{H}\end{pmatrix} + \mathbf{K}^2\begin{pmatrix}\mathbf{E}\\ \mathbf{H}\end{pmatrix} = 0, \tag{3}$$

$$\nabla\times\begin{pmatrix}\mathbf{E}\\ \mathbf{H}\end{pmatrix} = \mathbf{K}\begin{pmatrix}\mathbf{E}\\ \mathbf{H}\end{pmatrix}, \tag{4}$$

$$\nabla\cdot\begin{pmatrix}\mathbf{E}\\ \mathbf{H}\end{pmatrix} = 0, \tag{5}$$

where

$$\mathbf{K} = \frac{q_c}{1 - q_c^2\beta_c^2}\begin{pmatrix} q_c\beta_c & iZ_c \\ -iZ_c^{-1} & q_c\beta_c \end{pmatrix}, \tag{6}$$

with $Z_c = \sqrt{\mu_c\mu_0/(\epsilon_c\epsilon_0)}$ and $q_c = \omega\sqrt{\epsilon_c\mu_c}/c$, $c = 1/\sqrt{\epsilon_0\mu_0}$ being the velocity of light in vacuum.

A linear transformation of the EM field[16]

$$\begin{pmatrix} \mathbf{E} \\ \mathbf{H} \end{pmatrix} = \mathbf{A}\begin{pmatrix} \mathbf{Q}_L \\ \mathbf{Q}_R \end{pmatrix}, \tag{7}$$

with

$$\mathbf{A} = \begin{pmatrix} 1 & -iZ_c \\ -iZ_c^{-1} & 1 \end{pmatrix}, \tag{8}$$

diagonalizes $\mathbf{K}$, i.e.,

$$\mathbf{A}^{-1}\mathbf{K}\mathbf{A} = \begin{pmatrix} q_L & 0 \\ 0 & -q_R \end{pmatrix}, \tag{9}$$

where

$$q_L = q_c/(1 - q_c\beta_c), \tag{10}$$

$$q_R = q_c/(1 + q_c\beta_c). \tag{11}$$

The so-called Beltrami (transformed) fields, $\mathbf{Q}_L$ and $\mathbf{Q}_R$, satisfy Maxwell equations in the homogeneous chiral medium and the EM field can be decomposed into two eigenmodes corresponding to left- and right-circularly polarized waves, denoted by LCP and RCP, respectively. In a source-free medium with $\exp(-i\omega t)$ time dependence we have

$$\nabla^2\mathbf{Q} + \lambda^2\mathbf{Q} = 0, \tag{12}$$

$$\nabla \times \mathbf{Q} = \lambda\mathbf{Q}, \tag{13}$$

$$\nabla \cdot \mathbf{Q} = 0, \tag{14}$$

where $\lambda = q_L$ for $\mathbf{Q} = \mathbf{Q}_L$ and $\lambda = -q_R$ for $\mathbf{Q} = \mathbf{Q}_R$.

It can be readily verified that Eqs. (12)–(14) accept LCP and RCP plane-wave solutions of the form $\exp(i\mathbf{q}_L \cdot \mathbf{r})\hat{\mathbf{e}}_L$ and $\exp(i\mathbf{q}_R \cdot \mathbf{r})\hat{\mathbf{e}}_R$, where q_L and q_R are given by Eqs. (10) and (11), and $\hat{\mathbf{e}}_L$ and $\hat{\mathbf{e}}_R$ are unit vectors defined by $\hat{\mathbf{e}}_L = (\hat{\mathbf{e}}_{1L} + i\hat{\mathbf{e}}_{2L})/\sqrt{2}$ and $\hat{\mathbf{e}}_R = (\hat{\mathbf{e}}_{1R} - i\hat{\mathbf{e}}_{2R})/\sqrt{2}$ with each set of unit vectors $(\hat{\mathbf{e}}_{1L},\hat{\mathbf{e}}_{2L},\hat{\mathbf{q}}_L)$ and $(\hat{\mathbf{e}}_{1R},\hat{\mathbf{e}}_{2R},\hat{\mathbf{q}}_R)$ forming an orthogonal right-handed triad. Similarly, it is straightforward to show that the corresponding spherical-wave solutions have the form[17] $j_l(q_Lr)\mathbf{X}_{lm}(\hat{\mathbf{r}}) + \frac{1}{q_L}\nabla \times j_l(q_Lr)\mathbf{X}_{lm}(\hat{\mathbf{r}})$ and $j_l(q_Rr)\mathbf{X}_{lm}(\hat{\mathbf{r}}) - \frac{1}{q_R}\nabla \times j_l(q_Rr)\mathbf{X}_{lm}(\hat{\mathbf{r}})$, respectively, where j_l are spherical Bessel functions and $\mathbf{X}_{lm}(\hat{\mathbf{r}})$ are vector spherical harmonics. From the Beltrami fields, in either the plane-wave or the spherical-wave representation, one can obtain the corresponding EM field by Eq. (7).

In a usual lossless chiral medium, the limitation of the dimensionless chirality parameter $|q_c\beta_c|$ to values less than unity ensures positive wave numbers q_L and q_R, and positive energy density. However, this restriction is not necessary[4] and if the medium exhibits strong dispersion, $|q_c\beta_c|$ can be larger than unity in certain frequency regions, an example being chiral metamaterials.[9–11]

III. SCATTERING BY A CHIRAL SPHERE

We assume a homogeneous chiral sphere of radius S, characterized by EM parameters ϵ_c, μ_c, and β_c embedded in a nonchiral host medium characterized by ϵ and μ. The sphere is illuminated by a plane EM wave. Expanding the Beltrami fields inside the sphere into LCP and RCP vector spherical waves with expansion coefficients a^c_{Llm} and a^c_{Rlm}, respectively, we obtain the corresponding EM field through Eq. (7)

$$\mathbf{E}_{\text{in}}(\mathbf{r}) = \sum_{l=1}^{\infty}\sum_{m=-l}^{l}\left\{a^c_{Llm}\left[j_l(q_Lr)\mathbf{X}_{lm}(\hat{\mathbf{r}}) + \frac{1}{q_L}\nabla \times j_l(q_Lr)\mathbf{X}_{lm}(\hat{\mathbf{r}})\right] - iZ_ca^c_{Rlm}\left[j_l(q_Rr)\mathbf{X}_{lm}(\hat{\mathbf{r}}) - \frac{1}{q_R}\nabla \times j_l(q_Rr)\mathbf{X}_{lm}(\hat{\mathbf{r}})\right]\right\}, \tag{15}$$

$$\mathbf{H}_{\text{in}}(\mathbf{r}) = -iZ_c^{-1}\sum_{l=1}^{\infty}\sum_{m=-l}^{l}\left\{a^c_{Llm}\left[j_l(q_Lr)\mathbf{X}_{lm}(\hat{\mathbf{r}}) + \frac{1}{q_L}\nabla \times j_l(q_Lr)\mathbf{X}_{lm}(\hat{\mathbf{r}})\right] + iZ_ca^c_{Rlm}\left[j_l(q_Rr)\mathbf{X}_{lm}(\hat{\mathbf{r}}) - \frac{1}{q_R}\nabla \times j_l(q_Rr)\mathbf{X}_{lm}(\hat{\mathbf{r}})\right]\right\}. \tag{16}$$

Outside the sphere we express the EM field as a combination of the incident and scattered fields in the usual manner[18]

$$\mathbf{E}_{\text{out}}(\mathbf{r}) = \sum_{l=1}^{\infty}\sum_{m=-l}^{l}\left[\frac{i}{q}a^0_{Elm}\nabla \times j_l(qr)\mathbf{X}_{lm}(\hat{\mathbf{r}}) + a^0_{Hlm}j_l(qr)\mathbf{X}_{lm}(\hat{\mathbf{r}}) + \frac{i}{q}a^+_{Elm}\nabla \times h^+_l(qr)\mathbf{X}_{lm}(\hat{\mathbf{r}}) + a^+_{Hlm}h^+_l(qr)\mathbf{X}_{lm}(\hat{\mathbf{r}})\right], \tag{17}$$

$$\mathbf{H}_{\text{out}}(r) = Z^{-1}\sum_{l=1}^{\infty}\sum_{m=-l}^{l}\left[a^0_{Elm}j_l(qr)\mathbf{X}_{lm}(\hat{\mathbf{r}}) - \frac{i}{q}a^0_{Hlm}\nabla \times j_l(qr)\mathbf{X}_{lm}(\hat{\mathbf{r}}) + a^+_{Elm}h^+_l(qr)\mathbf{X}_{lm}(\hat{\mathbf{r}}) - \frac{i}{q}a^+_{Hlm}\nabla \times h^+_l(qr)\mathbf{X}_{lm}(\hat{\mathbf{r}})\right], \tag{18}$$

where $q = \omega\sqrt{\epsilon\mu}/c$, $Z = \sqrt{\mu\mu_0/(\epsilon\epsilon_0)}$, and h_l^+ are spherical Hankel functions, and the coefficients a^0_{Plm} and a^+_{Plm} ($P = E, H$) refer to the incident and scattered waves, respectively. Applying the proper boundary conditions, i.e., continuity of the tangential components of the EM field at the surface of the sphere, one can relate the expansion coefficients of the scattered field to those of the incident field through the so-called scattering T matrix

$$a^+_{Plm} = \sum_{P'=E,H} T_{PP';l}\, a^0_{P'lm}, \qquad P = E, H. \tag{19}$$

Explicit expressions for the elements of the T matrix, which is diagonal in l and independent on m because of the spherical symmetry, can be written as follows:[3]

$$T_{EE;l} = \frac{U_{L;l}C_{R;l} + U_{R;l}C_{L;l}}{U_{L;l}V_{R;l} + U_{R;l}V_{L;l}}, \tag{20}$$

$$T_{HH;l} = \frac{V_{L;l}D_{R;l} + V_{R;l}D_{L;l}}{U_{L;l}V_{R;l} + U_{R;l}V_{L;l}}, \tag{21}$$

$$T_{EH;l} = i\frac{U_{L;l}D_{R;l} - U_{R;l}D_{L;l}}{U_{L;l}V_{R;l} + U_{R;l}V_{L;l}} = -T_{HE;l}, \tag{22}$$

where

$$U_{L(R);l} = \sqrt{\frac{\epsilon_c\mu}{\epsilon\mu_c}}h_l^+(qS)\frac{1}{z}\frac{\partial[zj_l(z)]}{\partial z}\bigg|_{z=q_{L(R)}S} - j_l(q_{L(R)}S)\frac{1}{z}\frac{\partial[zh_l^+(z)]}{\partial z}\bigg|_{z=qS}, \tag{23}$$

$$V_{L(R);l} = h_l^+(qS)\frac{1}{z}\frac{\partial[zj_l(z)]}{\partial z}\bigg|_{z=q_{L(R)}S} - \sqrt{\frac{\epsilon_c\mu}{\epsilon\mu_c}}j_l(q_{L(R)}S)\frac{1}{z}\frac{\partial[zh_l^+(z)]}{\partial z}\bigg|_{z=qS}, \tag{24}$$

$$C_{L(R);l} = \sqrt{\frac{\epsilon_c\mu}{\epsilon\mu_c}}j_l(q_{L(R)}S)\frac{1}{z}\frac{\partial[zj_l(z)]}{\partial z}\bigg|_{z=qS} - j_l(qS)\frac{1}{z}\frac{\partial[zj_l(z)]}{\partial z}\bigg|_{z=q_{L(R)}S}, \tag{25}$$

$$D_{L(R);l} = j_l(q_{L(R)}S)\frac{1}{z}\frac{\partial[zj_l(z)]}{\partial z}\bigg|_{z=qS} - \sqrt{\frac{\epsilon_c\mu}{\epsilon\mu_c}}j_l(qS)\frac{1}{z}\frac{\partial[zj_l(z)]}{\partial z}\bigg|_{z=q_{L(R)}S}. \tag{26}$$

It can be seen that the T matrix is nondiagonal in P in the given representation, which reflects the mixing of the E- and H-polarization modes upon scattering because of chirality. The 2×2 blocks of the T matrix for given l have the form $\left(\begin{smallmatrix} A & B \\ -B & C \end{smallmatrix}\right)$ [see Eqs. (20)–(22)], and thus the corresponding eigenvalues are $\lambda_{l,\pm} = [(A + C) \pm \sqrt{(A - C - 2B)(A - C + 2B)}\,]/2$.

With the help of the T matrix, defined above, one can calculate directly the change in the number of states up to a frequency ω between the system under consideration (a single chiral sphere in a nonchiral host medium) and that of the host medium extending over all space[19]

$$\Delta N(\omega) = \frac{1}{\pi}\mathrm{Im}\ln\det[\mathbf{I} + \mathbf{T}] = \frac{1}{\pi}\mathrm{Im}\sum_{l=1}^{\infty}(2l+1)[\ln(1+\lambda_{l+}) + \ln(1+\lambda_{l-})] = \sum_{l=1}^{\infty}\Delta N_l(\omega), \tag{27}$$

where $\mathbf{I}$ is the unit matrix. Of more interest is the difference in the density of states induced by the scatterer and given by $\Delta n(\omega) = d\Delta N(\omega)/d\omega$. On the other hand, the scattering cross section associated with an LCP or RCP incident plane wave, normalized to the geometric cross section, can also be expressed in terms of the T matrix as follows:[20]

$$\sigma_{sc;L} = \frac{2}{(qS)^2}\sum_{l}^{\infty}(2l+1)\{|T_{EE;l}|^2 + |T_{HH;l}|^2 + 2|T_{EH;l}|^2 - 2\mathrm{Im}[(T_{EE;l} + T_{HH;l})T^*_{HE;l}]\}, \tag{28}$$

$$\sigma_{sc;R} = \frac{2}{(qS)^2}\sum_{l}^{\infty}(2l+1)\{|T_{EE;l}|^2 + |T_{HH;l}|^2 + 2|T_{EH;l}|^2 + 2\mathrm{Im}[(T_{EE;l} + T_{HH;l})T^*_{HE;l}]\}. \tag{29}$$

Let us consider, as an example, a single sphere of radius $S = 0.45a_0$ (a_0 here is an arbitrary length unit) made of a chiral material with $\beta_c/a_0 = 0.2$, $\epsilon_c = 2$, and $\mu_c = 1$ embedded in a nonchiral dielectric medium with $\epsilon = 3$ and $\mu = 1$. To scale with reality, assuming for the chirality parameter β_c a value of 3×10^{-8} m,[13] a_0 corresponds to 150 nm. This sphere supports resonant modes of the EM field, which are mostly localized at the sphere and leak to some minor degree in the host region. These modes are associated with the poles of the eigenvalues of the scattering T matrix in the lower complex frequency half-plane close to the real axis. Such poles appear for one of the eigenvalues of the T matrix as $q_c\beta_c$ approaches unity (and consequently q_L increases asymptotically) at $z_{il} = \omega_{il} - i\gamma_{il}$; ω_{il} is the eigenfrequency and γ_{il} ($0 < \gamma_{il} \ll \omega_{il}$) denotes the inverse of the lifetime of the respective 2^l-pole resonant mode of ith order. Considering the asymptotic expansions of the spherical Bessel functions for large arguments in the limit $q_LS \to \infty$, we deduce an approximate standing-wave-like condition for the occurrence of resonant modes: $q_LS - l\pi/2 + \varphi_l = n\pi$ for $n = 0, \pm 1, \pm 2, \ldots$, where φ_l are appropriate phase functions, which vary slowly with frequency for each value of l ($l = 1,2,3, \ldots$). Of course, the closer we get to the limit $q_c\beta_c \to 1$ the better the above approximation becomes.

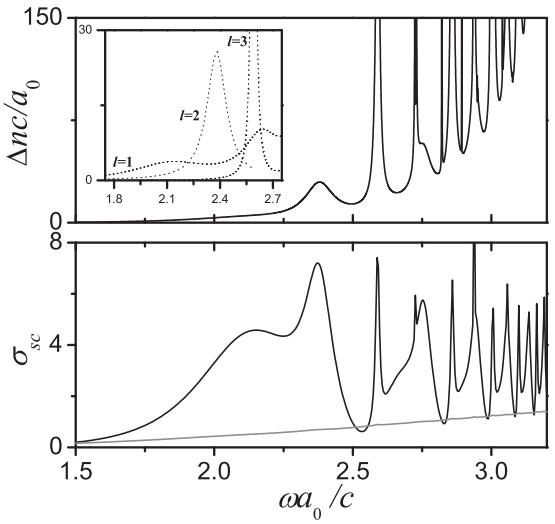

FIG. 1. The change in the density of states, Δn, induced by a single sphere of radius $S = 0.45a_0$ (a_0 here is an arbitrary length unit) made of a chiral material with $\beta_c/a_0 = 0.2$, $\epsilon_c = 2$, and $\mu_c = 1$ embedded in a nonchiral dielectric medium with $\epsilon = 3$ and $\mu = 1$ (upper diagram) and the corresponding scattering cross sections (lower diagram) associated with LCP (black line) and RCP (gray line) incident light. The inset to the upper diagram displays the symmetry-resolved resonant modes ($l = 1, 2, 3$, dotted lines) in the low-frequency part of the spectrum.

In the upper diagram of Fig. 1, we depict the change in the density of states, Δn, induced by the chiral sphere under consideration, calculated from Eq. (27). The inset to the diagram displays an enlarged view in the frequency region of the first resonant modes. It can be seen that Δn is characterized by resonance peaks and is nicely fitted by Lorentzian curves given by[19]

$$\Delta n_{il}(\omega) \approx \frac{2l+1}{\pi} \frac{\gamma_{il}}{(\omega-\omega_{il})^2+\gamma_{il}^2}, \quad i = 1,2,\ldots \tag{30}$$

The first two dipole ($l = 1$) resonant modes with lifetimes $\gamma_{11}^{-1}c/a_0 \cong 4$ and $\gamma_{21}^{-1}c/a_0 \cong 10$ appear at $\omega_{11} = 2.152c/a_0$ and $\omega_{21} = 2.651c/a_0$, respectively, while the first quadrupole ($l = 2$) mode appears at $\omega_{12} = 2.380c/a_0$ with $\gamma_{12}^{-1}c/a_0 \cong 16$ and the first octapole ($l = 3$) mode at $\omega_{13} = 2.380c/a_0$ with $\gamma_{13}^{-1}c/a_0 \cong 135$. As shown in the lower diagram of Fig. 1, these particle resonances can be excited solely by an LCP incident wave.

IV. A FACE-CENTERED CUBIC CRYSTAL OF CHIRAL SPHERES

We now consider an fcc crystal (with lattice constant a) of spheres embedded in a dielectric medium characterized by $\epsilon = 3$ and $\mu = 1$. We view the crystal as a sequence of (001) crystallographic planes. In each plane, the spheres are arranged on a square lattice with lattice constant $a_0 = a\sqrt{2}/2$ while consecutive planes are separated by a distance $d = a/2$. The spheres have a radius $S = 0.45a_0$ and are made of a chiral material with $\epsilon_c = 2$, $\mu_c = 1$, and $\beta_c/a_0 = 0.2$. It is interesting to note that the given crystal lacks invariance under space inversion because of its chiral constituents. Therefore, the appropriate point symmetry group is O, which consists of only proper rotations, and not O_h, that would be if the spheres were optically inactive.[21]

We study the photonic eigenmodes and the optical response of this crystal by means of full electrodynamic calculations using the layer-multiple-scattering method,[22,23] which is ideally suited for the case under consideration. Besides the complex photonic band structure of the infinite crystal, the method allows one to calculate, also, the reflectance of the semi-infinite crystal, $\mathcal{R}$, as well as the reflectance and transmittance of a finite slab of the crystal, at any angle and, in this respect, it can describe an actual transmission experiment. Another advantage of the method is that it solves Maxwell equations in the frequency domain and, therefore, it can treat dispersive materials, such as chiral substances, and include losses in a straightforward manner. The properties of the individual scatterers enter only through the corresponding T matrix. At a first step, in-plane multiple scattering is evaluated in the spherical-wave basis using proper propagator functions. Subsequently, interlayer scattering is calculated in a plane-wave basis through appropriate transmission and reflection matrices, by including all propagating and evanescent components of the wave field necessary to obtain convergence. Therefore, interaction between the scatterers is fully taken into account. The scattering S matrix of a multilayer slab, which transforms the incident into the outgoing wave field, is obtained by combining the transmission and reflection matrices of the component layers. The ratio of the transmitted or reflected energy flux to the energy flux associated with the incident wave defines the transmittance or reflectance of the slab, respectively. On the other hand, for a three-dimensional crystal consisting of an infinite periodic sequence of layers, stacked along the z direction, applying the Bloch condition for the wave field in the region between two consecutive unit slabs leads to an eigenvalue equation, which gives the z component of the Bloch wave vector, k_z, for the given frequency ω and in-plane wave-vector component reduced within the surface Brillouin zone, $\mathbf{k}_\parallel$, which are conserved quantities in the scattering process. The eigenvalues $k_z(\omega,\mathbf{k}_\parallel)$, looked upon as functions of real ω, define, for each $\mathbf{k}_\parallel$, lines in the complex k_z plane. Taken together they constitute the complex band structure of the infinite crystal associated with the given crystallographic plane. A line of given $\mathbf{k}_\parallel$ may be real (in the sense that k_z is real) over certain frequency regions and be complex (in the sense that k_z is complex) for ω outside these regions. It turns out that, for given $\mathbf{k}_\parallel$ and ω, out of the eigenvalues $k_z(\omega,\mathbf{k}_\parallel)$ none or, at best, a few are real and the corresponding eigenvectors represent propagating modes of the EM field in the given infinite crystal. The remaining eigenvalues $k_z(\omega,\mathbf{k}_\parallel)$ are complex and the corresponding eigenvectors represent evanescent waves. These have an amplitude, which increases exponentially in the positive or negative z direction, and, unlike the propagating waves, do not exist as physical entities in the infinite crystal. However, they are an essential part of the physical solutions of the EM field in a slab of finite thickness. A region of frequency where propagating waves do not exist for given $\mathbf{k}_\parallel$, constitutes a frequency gap of the EM field for the given $\mathbf{k}_\parallel$. If over a frequency region no propagating wave exists whatever the value of $\mathbf{k}_\parallel$, then this region constitutes an absolute frequency gap. In order

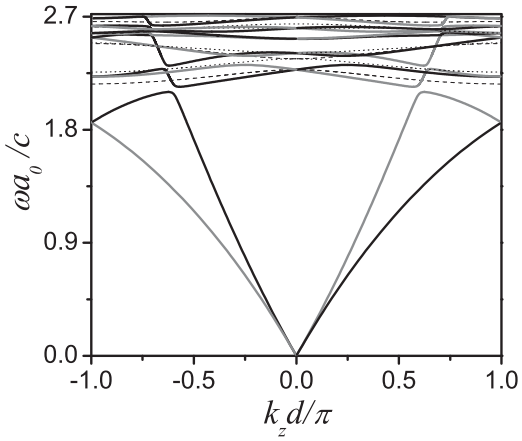

FIG. 2. The photonic band structure of an fcc crystal, with lattice constant a (nearest-neighbor distance, $a_0 = a\sqrt{2}/2$) of spheres of radius $S = 0.45a_0$ made of a chiral material with $\beta_c/a_0 = 0.2, \epsilon_c = 2$, and $\mu_c = 1$ embedded in a nonchiral dielectric medium with $\epsilon = 3$ and $\mu = 1$ along the [001] direction. The bands of LCP and RCP eigenmodes are shown by black and gray solid lines, respectively. With dashed and dotted lines we denote inactive bands (see also Fig. 3).

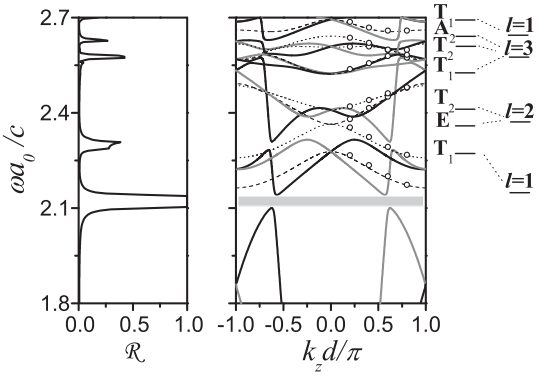

FIG. 3. A detailed view of Fig. 2 over a limited frequency region about the lowest multipole resonances of the single sphere, shown in the margin together with the corresponding eigenmodes at the center of the Brillouin zone. The latter are denoted by the appropriate irreducible representation of the relevant point group (the O group). The bands along the given [001] direction have the symmetry of the C_4 group: A (dashed line), B (dotted line), E_1 (black solid line), and E_2 (gray solid line). The shaded area marks the frequency gap. The open circles show the eigenfrequencies of a (001) slab of the given crystal, four-layers thick, plotted against discrete values of $k_z d/\pi = 1/5, 2/5, 3/5, 4/5$ (see text). On the left of the band diagram we display the corresponding reflection spectrum (for LCP and RCP incident waves) of the semi-infinite crystal.

to ensure adequate convergence in our calculations for the structure under consideration, it is sufficient to truncate the spherical-wave expansions at $l_{\max} = 6$ and take into account 37 two-dimensional reciprocal lattice vectors in the relevant plane-wave expansions.[22,23]

In Fig. 2 we display the calculated photonic band structure of the given crystal along its [001] direction. The bands along this direction can be classified according to the irreducible representations (A, B, E_1, E_2) of the C_4 group, which is a subgroup of O.[21] All these bands are nondegenerate since the irreducible representations of C_4 are one dimensional. The E_1 and E_2 bands have the symmetry of LCP and RCP propagating waves, respectively, and thus can be excited by a wave of the appropriate polarization, incident normally on the (001) surface of the crystal. The A and B bands cannot be excited by an externally incident wave because they do not have the proper symmetry. These bands correspond to bound states of the EM field in a finite (001) slab of the crystal, which decrease exponentially outside the slab on either side of it. To demonstrate this, we determined the eigenmodes of a (001) slab of the given crystal consisting of $N_L = 4$ planes of spheres for $\mathbf{k}_\parallel = (0,0)$ in the manner of Ref. 24. Over the frequency range of each of these bands we obtain four eigenfrequencies, which when plotted against values of the reduced wave number $k_z = \kappa\pi/(N_L + 1)$, where $\kappa = 1,2,\ldots,N_L$ and $N_L = 4$, reproduce the corresponding dispersion curves of the infinite crystal as shown by the open circles in Fig. 3.

The eigenmodes at the center of the Brillouin zone, $\mathbf{k} = (0,0,0)$, have the symmetry of the full O point group, while at the boundaries of the Brillouin zone, $\mathbf{k} = (0,0,\pm\pi/d)$, they have the symmetry of the D_4 point group, which is a subgroup of O. Compatibility between the irreducible representations of the O and C_4 and of the D_4 and C_4 groups (see Table I) implies that the optically active LCP and RCP bands along the [001] direction, of E_1 and E_2 symmetry, respectively, converge to doubly degenerate modes of E symmetry at the corresponding boundaries of the Brillouin zone and to three-fold degenerate (T_1 or T_2) modes at the center of the Brillouin zone, as shown in Fig. 3. Another interesting feature in the band diagram of Figs. 2 and 3 follows from invariance under time reversal, which reflects reciprocity as in the case of nonchiral photonic crystals: though $\omega_{nE_1}(\mathbf{k}) \neq \omega_{nE_1}(-\mathbf{k})$ and $\omega_{nE_2}(\mathbf{k}) \neq \omega_{nE_2}(-\mathbf{k})$, because of the lack of space-inversion symmetry $\omega_{nE_1}(\mathbf{k}) = \omega_{nE_2}(-\mathbf{k})$, where $n = 1,2,\ldots$ is a band index. This means that time-reversal symmetry *alone* ensures degeneracy of the LCP and RCP modes at the center and the boundaries of the Brillouin zone. We note that polarization decomposition and existence of optically inactive bands apply along high-symmetry directions, such as [001] or [111]. Along an arbitrary direction, all bands belong to the identity representation and thus can be excited by an appropriately incident wave of any polarization.

At low frequencies (below $\omega a_0/c \approx 2$) we obtain nondegenerate extended bands of LCP and RCP modes of E_1 and E_2 symmetry, respectively, as expected for propagation in a homogeneous chiral effective medium in the reduced zone representation because of structure periodicity. At higher frequencies, the dispersion diagram is characterized by the narrow bands, which originate from the resonant modes of the individual spheres, weakly interacting between them. The E_1 and E_2 components of these resonance bands interact with the extended effective medium bands of the same symmetry to produce the band structure shown in Figs. 2 and 3. It can be seen that anticrossing interactions lead to strong band bending and negative-slope dispersion inside the Brillouin zone while a frequency gap extending from $\omega a_0/c = 2.103$

TABLE I. Compatibility relations between the irreducible representations of the O and C_4, and of the D_4 and C_4 groups.

O	A_1	A_2	E	T_1	T_2
C_4	A	B	$A\ B$	$A\ E_1\ E_2$	$B\ E_1\ E_2$
D_4	A_1	B_1	A_2	B_2	E
C_4	A	B	A	B	$E_1\ E_2$

to $\omega a_0/c = 2.139$ opens up along the [001] direction of the given crystal.

We note that the total number of bands shown in Fig. 2 equals the number expected from the interaction of the resonance bands with the "would be" extended effective medium bands. In agreement with group theory (see also Table I), as can be seen in Fig. 3, a dipole resonant mode of the individual spheres gives a threefold degenerate mode of T_1 symmetry at the center of the Brillouin zone, which splits into an A, an E_1, and an E_2 band along the [001] direction. Correspondingly, a quadrupole resonant mode gives a doubly degenerate E mode and a threefold degenerate T_2 mode at $\mathbf{k} = (0,0,0)$. These are separated into an A and a B band and into a B and an E_1 and an E_2 band along the [001] direction, respectively. Moreover, an octapole resonant mode of the spheres gives a nondegenerate A_2 mode as well as two threefold degenerate modes of T_1 and T_2 symmetry at $\mathbf{k} = (0,0,0)$. Along the [001] direction, these evolve as: a B band; an E_1, an E_2, and an A band; an E_1, an E_2, and a B band, respectively.

Next to the band-structure diagram, in Fig. 3 we also depict the reflection spectrum of the corresponding semi-infinite crystal, for light incident normally on its (001) surface. We find that the reflectance does not depend on the polarization (LCP or RCP) of the incident wave, as in the case of a homogeneous chiral medium.[25,26] It is interesting to note that the existence of only RCP (LCP) modes for positive (negative) k_z, e.g., above and below the frequency gap (see Figs. 2 and 3), does not mean polarization-selective transmission. Indeed, light propagation along a given direction in the crystal occurs through those bands with the proper sign of their group velocity (forward-propagating modes) and not of k_z. As can be seen from Figs. 2 and 3, an RCP band with positive or negative group velocity at a given frequency is accompanied by an LCP band with the same sign of group velocity at this frequency and vice versa. Therefore, circularly polarized waves of either handedness can be transmitted through the crystal. In the gap region, where propagating modes of the EM field in the crystal are absent, the reflectance equals unity as shown in the left-hand diagram of Fig. 3.

As mentioned above, along an arbitrary direction, all bands belong to the identity representation and thus can be excited by an appropriately incident wave of any polarization. However, since the bands couple to a different degree with each polarization mode, the corresponding reflection spectrum for LCP and RCP incident light is, in this case, different, as shown in Fig. 4.

Losses in a chiral medium, which are significant for chiral metamaterials, imply an imaginary part also in the chirality parameter and can be taken into account in our calculations.

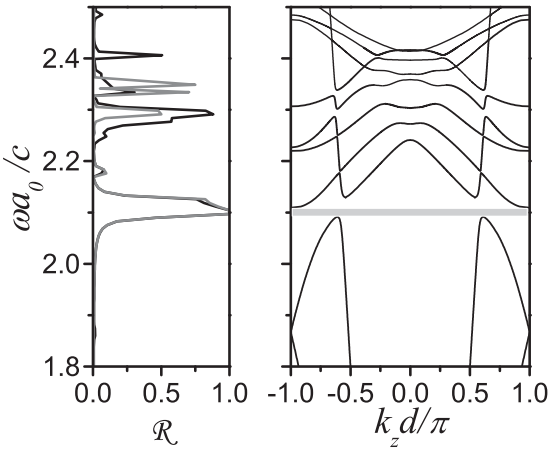

FIG. 4. The photonic band structure of the crystal under consideration, for $\mathbf{k}_\parallel = (0.1,0)2\pi/a_0$. The shaded area marks the frequency gap. On the left of the band diagram we display the corresponding reflection spectrum of the semi-infinite crystal for LCP (black line) and RCP (gray line) incident light.

Losses cause all bands to become complex, in the sense that all values of the wave vector acquire an imaginary part, and reduce the reflection peaks because of absorption.

In our calculations, we assumed that the different EM parameters of the constituent materials are constants over the range of frequency considered but our method can deal with situations in which these parameters depend on the frequency. It should be pointed out that, assuming a constant value for β_c, the strength of chirality, described by the dimensionless parameter $|q_c\beta_c|$, vanishes at the static limit ($\omega = 0$) and increases linearly with frequency; this allows us to study both the weak- and strong-chirality regimes in the same physical system. In the frequency region of interest, i.e., about $\omega a_0/c \approx 2.5$, the constant chirality parameter $\beta_c = 0.2a_0$ that we assumed corresponds to $q_c\beta_c \approx 0.7$, which is achievable in practice. In chiral metamaterials, $|q_c\beta_c|$ can even exceed unity near a resonance frequency, leading to a negative effective refractive index for a specific polarization mode.[9–11] Moreover, there are substances with very strong chirality, an example being helical polymers. For instance, it has been reported that poly-L-lactic acid (PLLA) exhibits a huge optical rotatory power,[27] which corresponds to $\beta_c = 3.08 \times 10^{-8}$ m.[13] Therefore, PLLA nanoparticles,[28] self-assembled into an ordered structure, could offer a route for the realization of crystals of chiral spheres such as that studied in the present work, operating at optical frequencies.

V. CONCLUSIONS

In summary, we reported a thorough investigation of the optical eigenmodes and light propagation in three-dimensional periodic structures of chiral spheres in a nonchiral medium, by means of rigorous, full electrodynamic calculations using the layer-multiple-scattering method. We analyzed dispersion diagrams in conjunction with corresponding reflection spectra and explained aspects of the underlying physics to a degree that goes beyond existing interpretation. In the strong chirality

regime, but below the negative-index threshold, resonant modes of the individual spheres, weakly interacting with each other, form slow-light bands that hybridize with the other photonic modes of the appropriate symmetry. Our results reveal a rich photonic band structure, which exhibits remarkable features that endow these composites with functionalities such as slow-light transport, splitting of circular polarization states, and filtering. Moreover, we reported a rigorous group theory analysis for the proper characterization of all eigenmodes according to their symmetry, which complements previous work on the subject[14] and is also useful for the interpretation of photonic band diagrams of chiral metamaterials.[12]

ACKNOWLEDGMENT

A. Christofi was supported by NCSR "Demokritos" through a postgraduate fellowship.

*aristi@ims.demokritos.gr

[1] K. M. Flood and D. L. Jaggard, J. Opt. Soc. Am. A **13**, 1395 (1996).
[2] J. Chongjun, Q. Bai, Y. Miao, and Q. Ruhu, Opt. Commun. **142**, 179 (1997).
[3] I. E. Psarobas, N. Stefanou, and A. Modinos, J. Opt. Soc. Am. A **16**, 343 (1999).
[4] S. Tretyakov, I. Nevedov, A. Sihvola, S. Maslovski, and C. Simovski, J. Electromagn. Waves. Appl. **17**, 695 (2003).
[5] C. Monzon and D. W. Forester, Phys. Rev. Lett. **95**, 123904 (2005).
[6] J. B. Pendry, Science **306**, 1353 (2004).
[7] V. Yannopapas, J. Phys. Condens. Matter **18**, 6883 (2006).
[8] J. K. Gansel, M. Thiel, M. S. Rill, M. Decker, K. Bade, V. Saile, G. von Freymann, S. Linden, and M. Wegener, Science **325**, 1513 (2009).
[9] S. Zhang, Y. S. Park, J. Li, X. C. Lu, W. Zhang, and X. Zhang, Phys. Rev. Lett. **102**, 023901 (2009).
[10] E. Plum, J. Zhou, J. Dong, V. A. Fedotov, T. Koschny, C. M. Soukoulis, and N. I. Zheludev, Phys. Rev. B **79**, 035407 (2009).
[11] X. Xiong, W. H. Sun, Y. J. Bao, M. Wang, R. W. Peng, C. Sun, X. Lu, J. Shao, Z. F. Li, and N. B. Ming, Phys. Rev. B **81**, 075119 (2010).
[12] C. Wu, H. Q. Li, Z. Wei, X. T. Yu, and C. T. Chan, Phys. Rev. Lett. **105**, 247401 (2010).
[13] C. He, M. H. Lu, R. C. Yin, T. Fan, and Y. F. Chen, J. Appl. Phys. **108**, 073103 (2010).
[14] F. Jonsson and C. Flytzanis, Phys. Rev. Lett. **97**, 193903 (2006).
[15] A. Lakhtakia, *Beltrami Fields in Chiral Media* (World Scientific, Singapore, 1994).
[16] C. F. Bohren, Chem. Phys. Lett. **29**, 458 (1974).
[17] J. D. Jackson, *Classical Electrodynamics* (Wiley, New York, 1998).
[18] N. Stefanou and A. Modinos, J. Phys. Condens. Matter **3**, 8135 (1991).
[19] G. Gantzounis, N. Stefanou, and V. Yannopapas, J. Phys. Condens. Matter **17**, 1791 (2005).
[20] C. F. Bohren and D. R. Huffman, *Absorption and Scattering of Light by Small Particles* (Wiley, New York, 1983).
[21] J. F. Cornwell, *Group Theory and Electronic Energy Bands in Solids* (North-Holland, Amsterdam, 1969).
[22] N. Stefanou, V. Yannopapas, and A. Modinos, Comput. Phys. Commun. **113**, 49 (1998).
[23] N. Stefanou, V. Yannopapas, and A. Modinos, Comput. Phys. Commun. **132**, 189 (2000).
[24] V. Karathanos, J. Mod. Opt. **45**, 1751 (1998).
[25] M. P. Silverman, J. Opt. Soc. Am. A **3**, 830 (1986).
[26] S. Bassiri, C. H. Papas, and N. Engheta, J. Opt. Soc. Am. A **5**, 1450 (1988).
[27] Y. Tajitsu, R. Hosoya, T. Maruyama, M. Aoki, Y. Shikinami, M. Date, and E. Fukada, J. Mater. Sci. Lett. **18**, 1785 (1999).
[28] H. X. Ge, Y. Hu, S. C. Yang, X. Q. Jiang, and C. Z. Yang, J. Appl. Polym. Sci. **75**, 874 (2000).